<u>**Electronic supplementary material**</u>

Demise of Marimermithida refines primary routes of transition to parasitism in roundworms

Alexei V. Tchesunov, Olga V. Nikolaeva, Leonid Yu. Rusin, Nadezda P. Sanamyan, Elena G. Panina, Dmitry M. Miljutin, Daria I. Gorelysheva, Anna N. Pegova, Maria R. Khromova, Maria V. Mardashova, Kirill V. Mikhailov, Vladimir V. Yushin, Nikolai B. Petrov, Vassily A. Lyubetsky, Mikhail A. Nikitin and Vladimir V. Aleoshin

1. Supplementary figures

Figure S1. ML tree of Nematoda based on combined SSU, 5.8S and LSU rDNA data. Nodes labelled with bootstrap support values estimated under GTR+F+G16 model in 100 replicates. Scale bar: substitutions per site.

Figure S2. Bayesian tree of Nematoda based on SSU rDNA data. Nodes labelled with posterior probabilities (%) calculated across GTR+Γ parameter space in 3 M generations. Consensus topology obtained with 50% burn-in. Scale bar: substitutions per site.
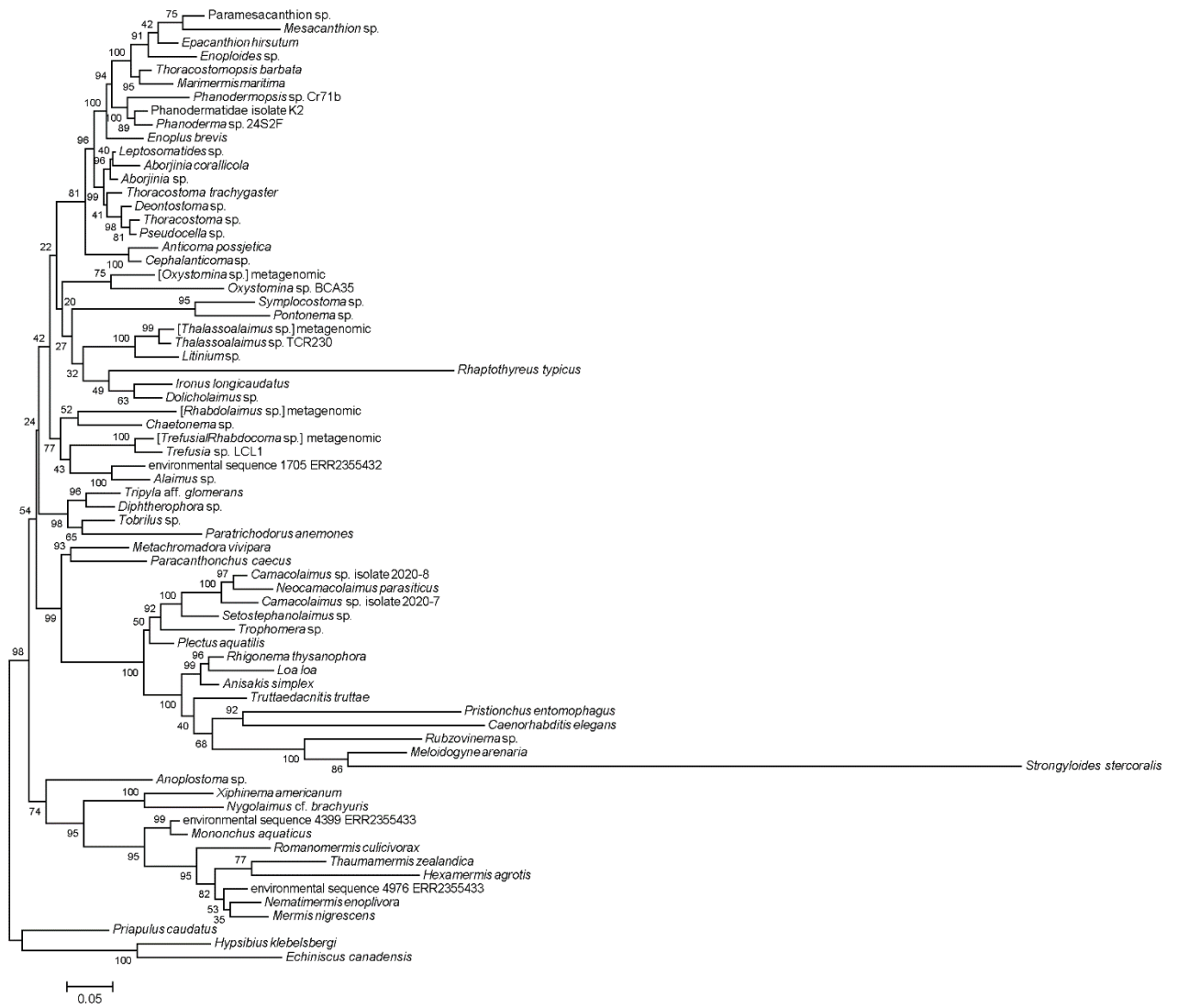
Figure S3. Bayesian tree of Nematoda based on LSU rDNA data. Nodes labelled with posterior probabilities (%) calculated across GTR+Γ parameter space in 3 M generations. Consensus topology obtained with 50% burn-in. Scale bar: substitutions per site.

2. Molecular data origin and availability

Sequences obtained originally in the study. NCBI GenBank accession IDs provided for genes. Raw NGS data available in NCBI BioProject PRJNA772260

Taxonomic unit	Method	BioSample	SSU	5.8S	LSU
Aborjinia sp. OVP-2021 isolate KKT	Sanger		MZ504143		
Anticoma possjetica	Sanger		MZ476002		
Camacolaimus sp. OVN-2021 isolate 2020-7	Sanger		OL416401		OL416398
Camacolaimus sp. OVN-2021 isolate 2020-8	Sanger		OL416400		OL416397
Marimermis maritima	Sanger		MZ504144		
Metachromadora vivipara	NGS	SAMN22371214	MZ476003	MZ504149	
Nematimermis enoplivora	Sanger		MZ476004		
Paracanthonchus caecus isolate Pc-OVN-2021	Sanger				OL416396
phanodermatidae gen. sp. OVP-2021 isolate K2	Sanger		MZ476005		MZ474687
Setostephanolaimus sp. isolate OVN-2021	Sanger		OL416402		OL416399
Thoracostoma sp. OVP-2021 isolate C-Tsp	NGS	SAMN22371215	MZ504146		
Thoracostomopsis barbata	NGS	SAMN22371216	MZ476006	MZ504147	
Tripyla aff. *glomerans* OVP-2021 isolate C-Tg	NGS	SAMN22371213	MZ504148		

Sequences originally assembled from third-party NGS data

Taxonomic unit	BioProject	SRA
Neocamacolaimus parasiticus	PRJNA707491	SRR13895039
[*Oxystomina* sp.] metagenomic	PRJNA415343	SRR6202057
[*Thalassoalaimus* sp.] metagenomic	PRJNA415343	SRR6202055
[*Trefusia / Rhabdocoma* sp.] metagenomic	PRJNA415343	SRR6202055
[*Rhabdolaimus* sp.] metagenomic	PRJNA336658	SRR4030105

Third-party NCBI GenBank gene accession IDs

Taxonomic unit	SSU	5.8S	LSU
Aborjinia corallicola voucher S11306-2	MW916782		MW916763
Alaimus sp. SK-2012			JN123432
Anisakis simplex	AB277822		
Anoplostoma sp. BUS21	HM564407		HM564663
Caenorhabditis elegans	X03680		
Cephalanticoma sp. TCR141	HM564612		HM564842
Chaetonema sp. NAR6	HM564431		HM564699

Cryptonchus tristis	EF207244		
Deontostoma sp. 1S2F8	FN433899		FN433915
Diphtherophora sp. Shahrood	KY115102		KY115123
Dolicholaimus sp. TCR114	HM564604		HM564836
Domorganus macronephriticus strain DoGaMac2	FJ969122		
Dracunculus medinensis isolate PDB18-022	MK163617		
Echiniscus canadensis isolate Tar14	FJ435713		FJ435785
Echinomermella matsi	HQ668023		
Enoploides sp. DBA1	HM564549		HM564757
Enoplus brevis	U88336		
Enoplus meridionalis	Y16914		
Epacanthion hirsutum	MG599065		GU139778
environmental sequence 1705	ERX2404076 / ERR2355432		
environmental sequence 4399	ERX2404077 / ERR2355433		
environmental sequence 4976	ERX2404077 / ERR2355433		
Hexamermis agrotis	DQ530350		KC784667
Hypsibius klebelsbergi voucher HD005	KT901827		KT901829
Ironus longicaudatus	FJ040495		
Leptosomatides sp. TCR192	HM564626		HM564855
Litinium sp. TCR90	HM564650		HM564875
Loa loa	XR_002251421		XR_002251420
Meloidogyne arenaria	U42342		
Mermis nigrescens isolate Mjuv	KF583882		KF886019
Mesacanthion sp. 2 TJP-2019 Nem.77	MN250061		
Mononchus aquaticus	AY297821		
Nygolaimus cf. *brachyuris* JH-2004	AY284770		AY593061
Oxystomina sp. BCA35	HM564494		HM564749
Paracanthonchus caecus	AF047888		
Paramesacanthion sp. 2 AAS-2018 isolate SB101	MK007609		MK007589
Paramphidelus hortensis	AY284739		
Paratrichodorus anemones	AF036600		AJ781505
Phanoderma sp. 24S2F	FN433904		FN433914
Phanoderma sp. AS484	KR265046		
Phanodermopsis sp. Cr66	HM564523		HM564884
Phanodermopsis sp. Cr71b	HM564525		HM564886
Plectus aquatilis	AF036602		EF417147
Pontonema sp.	Smythe et al. 2019		
Priapulus caudatus	Z38009	AY210840	
Pristionchus entomophagus	FJ040441		KT188873
Pseudocella sp. 3S26E8	FN433901		FN433910
Rhabdolaimus aquaticus	FJ969139		
Rhaptothyreus typicus	MG547378		MG547379
Romanomermis culicivorax	CAQS01000365		
Rubzovinema sp. EIK-2013	KF155281		
Soboliphyme baturini	AY277895		
Strongyloides stercoralis	M84229		KU180693

Symplocostoma sp.	Smythe et al. 2019	
Thalassoalaimus sp. TCR230	HM564634	HM564880
Thaumamermis zealandica	KY264164	KY264165
Thoracostoma trachygaster	FN433905	FN433917
Tobrilus sp.	Smythe et al. 2019	
Trefusia sp. LCL1	HM564576	HM564783
Trichinella spiralis	KC006424	
Trophomera sp. TAN1711	MH665402	MH665403
Truttaedacnitis truttae	EF180063	
Xiphinema americanum	AY580056	

Original assemblies by Smythe et al. 2019[ref.1] are available at https://figshare.com/s/4c8e501714dbd5be1be8

3. Supplementary Materials and Methods

3.1. Material extraction, processing and free-living nematodes collection

Host individuals of sea urchin *Strongylocentrotus polyacanthus* were opened unfixed, and specimens of *Marimermis maritima* collected from coelomic cavity and preserved with 96% ethanol for DNA extraction.

The host individual of *Priapulus caudatus* was dissected unfixed, and *Aborjinia* sp. specimen retrieved from introvert haemocoel onboard of the vessel. The nematode was divided in three parts; anterior and posterior ends were fixed with 10% buffered seawater formalin for light microscopy. The middle portion was subdivided in two; one part was fixed with 100% ethanol and stored at –20°C, another part – with DESS[2] and stored at room temperature; both parts were used for DNA extraction.

Host specimens of *Enoplus communis* were extracted from muddy inter- to subtidal sediment by repeated decantation and fine-sieving. The *Nematimermis enoplivora* parasite was retrieved live from body cavity of scalpel-punctured hosts, sliced and fixed with 96% ethanol for DNA extraction.

Foraminifers *Reophax curtus* were cavitation-extracted from muddy subtidal sediment of trawl catch and fixed with DESS. Individuals of Phanodermatidae and *Camacolaimus* spp. were isolated manually from fixed tests under stereo microscopes.

Specimens of *Paracanthonchus caecus*, *Thoracostomopsis barbata*, *Pseudocella trichodes*, *Thoracostoma* sp. and *Metachromadora vivipara* were sampled from subtidal sandy sediments near the White Sea Biological Station of Moscow State University, *Tripyla* sp. – from freshwater detrital debris of the Chernaya river bed in August 2018 (Kandalaksha Bay, White Sea). Nematodes were extracted by decantation-sieving and fixed with RNAlater stabilisation solution (Thermo Fisher Scientific, USA) for total RNA extraction. Individuals of *Anticoma possjetica*

were obtained from bivalve *Crenomytilus grayanus* clusters collected at a 10 m depth near the Vostok Biological Station of A.V. Zhirmunsky National Scientific Centre of Marine Biology in August 2004 (Vostok Bay, Sea of Japan); worms fixed with 96% ethanol for DNA extraction.

3.2. DNA/RNA extraction and sequencing

Individual nematodes were lysed in 20 µl proteinase K-containing buffer[3]. Total DNA was extracted with NucleoSpin Tissue XS kits (Macherey-Nagel, Germany) following a manufacturer protocol. PCR amplification of partial SSU (18S) rDNA, complete ITS regions and partial LSU (28S) rDNA was conducted with specific primers[4,5] using Encyclo PCR chemistry (Evrogen, Russia). PCR cycling: primary denaturation at 95°C for 5 min, cycle denaturation at 95°C for 30 s (40 cycles), annealing at 55°C for 30 s, extension at 72°C for 3 min, final extension at 72°C for 5 min. PCR products were agarose gel-purified with Cleanup Mini kits (Evrogen, Russia). Amplicons were sequenced directly with an Applied Biosystems 3730 DNA Analyzer (Thermo Fisher Scientific, USA). Original transcriptomic data was generated in *Metachromadora vivipara*, *Pseudocella trichodes*, *Thoracostomopsis barbata*, *Thoracostoma* sp. and *Tripyla glomerans*. Total RNA from nematode samples was extracted using Arcturus PicoPure RNA Isolation Kits (Thermo Fisher Scientific, USA). Transcriptomic libraries for *P. trichodes*, *T. barbata* and *Thoracostoma* sp. were prepared with the TruSeq protocol (Illumina, USA). In *M. vivipara* and *T. glomerans*, cDNA was synthesised with SMART-Seq v4 Ultra Low Input RNA Kits (Takara Bio, France). Libraries were sequenced on an Illumina HiSeq 4000 system, generating 16–37 M 150-bp paired-end reads for each sample. Original raw NGS data are deposited as NCBI BioProject PRJNA772260, rDNA cistron assemblies and original Sanger sequences are deposited in NCBI GenBank.

3.3. Dataset and phylogenetic pipeline

Illumina reads were processed with Trimmomatic[6] and *cutadapt*[7] tools to remove adapter sequences and assembled using SPAdes[8] with *k*-mer values 77 and 127. Contigs corresponding to rDNA operons were extracted from SPAdes assemblies using BLAST[9]. Fragmented rDNA operons were merged by overlapping contigs or contig termini, and the resulting operon assemblies were examined for errors by read mapping with Bowtie2[ref.10] and the mapping inspection in Tablet[11]. Additional rDNA sequences were obtained from the GenBank *nr*, *wgs*, SRA and *figshare* repositories (see above). Individual alignments of SSU, 5.8S and LSU rDNA were prepared with MAFFT[12] using Q-INS-i RNA secondary structure-aware algorithm. Variable indel-rich hairpin regions were additionally realigned by X-INS-i algorithm incorporating pairwise structural alignment by MXSCARNA[13] and using conserved flanking hairpins as alignment anchors. For

tree inference, the alignments were masked with trimAl[14] using the built-in automated trimming heuristic (-automated1). The alignment length was 1703 bp in SSU, 152 bp in 5.8S and 2390 bp in LSU rDNA. Three gene alignments were manually concatenated (90 taxa total) and used for tree inference as partitioned supermatrix or separately. Bayesian phylogenetic inference (BI) was performed using MrBayes 3.2.6[ref.15] with two runs (nst=6 ngammacat=16 rates=invgamma), three partitions (SSU, 5.8S, LSU), 3,000,000 generations and 50% burn-in. Average standard deviation of split frequencies was 0.4 on run completion. Runs converged across all parameters with PSRF[16] estimate 1.0. Maximum likelihood (ML) trees with bootstrap support were estimated in 100 replicates (–b 100) using IQ-TREE 1.6[17]. Best model was selected with ModelFinder (–m MF[18]) on topology fixed as BI consensus (–t). The best model initially selected according to BIC and AIC across partitions was GTR+F+G4; it was refined further with ModelFinder (–mset GTR+F) by explicitly testing rate heterogeneity types (–mrate) as G4, G6, G8, G10, G12, G14, G16 and G18. The GTR+F+G16 model was ultimately selected and used in downstream analyses. Phylogenetic trees were visualised with MEGA 6.0[ref.19]. Alternative hypothesis testing was performed according to the approximately unbiased (AU[ref.20]) and expected likelihood weight (ELW[21]) tests implemented in IQ-TREE 1.6. Hypotheses were formalised as topological constraints and used in ML inference with IQ-TREE under the model parameters pre-estimated as described above and 10,000 RELL replicates (–zb 10000) for bootstrap support approximation[22]. The constraint hypotheses and their related confidence values in a test tree set containing consensus ML and BI trees are detailed below in Section 3.4.

3.4. Statistical ML tests of phylogenetic hypotheses

ML-based hypothesis testing for monophyletic placement of the nematode lineages under study was performed as follows. The lineages with parasitic or other host-associated lifestyle were tested in pairwise combinations for exclusive monophyly against other nematode taxa (as test hypotheses) in a tree set containing all test hypotheses, including BI and ML consensus trees. Given the overall high-supported consensus trees, we reduced test combinatorics outside the primary subjects in Enoplia to only verity *Nematimermis enoplivora* for exclusion from Mermithida and Dorylaimia (hypotheses `N_OUT_MER` and `N_OUT_DOR`, respectively). Test hypotheses were formalised as topological constraints (ref. to table below) and used in ML inference with IQ-TREE 1.6. Approximately unbiased (`AU`, $p < 0.05$) and expected likelihood weight (`c-ELW`) statistical tests were used as implemented in IQ-TREE with 10,000 RELL replicates (`-zb 10000`) and GTR+F+G16 model pre-selected. Non-rejected hypotheses and respective confidence values are **in bold**. Abbreviations are self-explaining and provided for

clarity; `Nematoda, Dorylaimia, Mermithida` = the rest of dataset relative to the explicitly constrained taxa in each hypothesis.

All tests did not discriminate between the ML and BI trees. All pairwise hypotheses were rejected except for the grouping of *Rhaptothyreus typicus* with *Echinomermella matsi*. The latter exclusive monophyly is not rejected at a lower-boundary *p*-value in AU, rejected in ELW test and discords with the ML/BI topologies, which assertively suggests an uncertain volatile positioning of *R. typicus* and requires a separate methodological effort and/or further molecular evidence. The affinity of *N. enoplivora* to the outer tree with respect to both Mermithida and Dorylaimia is rejected, thus confirming its placement as a crown mermithid.

Test hypothesis	AU *p*-value	c-ELW
Bayesian consensus	0.518 +	0.498 +
Maximum likelihood consensus	0.625 +	0.476 +
AAM ((Aborjinia corallicola,*Aborjinia* sp.,*Marimermis maritima*),Nematoda);	6.26×10^{-45} –	6.35×10^{-113} –
AAP ((Aborjinia corallicola,*Aborjinia* sp.,phanodermatid K2),Nematoda);	5.42×10^{-46} –	1.76×10^{-104} –
AAE ((Aborjinia corallicola,*Aborjinia* sp.,*Echinomermella matsi*),Nematoda);	6.69×10^{-6} –	8.02×10^{-55} –
AAR ((Aborjinia corallicola,*Aborjinia* sp.,*Rhaptothyreus typicus*),Nematoda);	0.00802 –	0.00379 –
MP ((*Marimermis maritima*,phanodermatid K2),Nematoda);	2.14×10^{-71} –	1.67×10^{-70} –
ME ((*Marimermis maritima*,*Echinomermella matsi*),Nematoda);	6.09×10^{-5} –	2.51×10^{-39} –
MR ((*Marimermis maritima*,*Rhaptothyreus typicus*),Nematoda);	0.0166 –	0.00447 –
PE ((phanodermatid K2,*Echinomermella matsi*),Nematoda);	7.81×10^{-116} –	1.92×10^{-22} –
PR ((phanodermatid K2,*Rhaptothyreus typicus*),Nematoda);	1.89×10^{-5} –	9.41×10^{-8} –
ER ((*Echinomermella matsi,Rhaptothyreus typicus*),Nematoda);	**0.0861 +**	1.5×10^{-8} –
AAMR ((Aborjinia corallicola,*Aborjinia* sp.,*Marimermis maritima,Rhaptothyreus typicus*),Nematoda);	1.27×10^{-5} –	3.11×10^{-114} –
N_OUT_DOR ((Dorylaimia), *Nematimermis enoplivora*, Nematoda);	9.27×10^{-5} –	5.62×10^{-165} –
N_OUT_MER ((Mermithida), *Nematimermis enoplivora*, Nematoda);	0.0142 –	0.0178 –

4. Biological material identification

Detailed morphology and verification data for specimen identification in *Marimermis maritima*, *Aborjinia* sp. and phanodermatid K2.

4.1. Specimen identification in Marimermis maritima *(Figure 1, A)*

The specimen was identified to species level based on morphology and descriptive data from [23,24].

4.2. Specimen identification in Aborjinia *sp. (Figure 1, B)*

The specimen of *Aborjinia* sp. was identified to genus level based on morphological and metric data. Main measurements: L = ca. 30 mm; a = 60; b = 20; c = 74; c′ = 1.4. Body diameters at level of: second head sensilla circle = 109 μm; amphid = 126 μm; nerve ring = 250 μm; cardia = 290 μm; anus = 290 μm. Maximum diameter = ca. 500 μm. Body whitish, opaque, cylindrical, slightly narrowed towards anterior end. Tail short, in shape of rounded cone. Internal organs visible hardly due to fleshy body walls consisting of very developed hypodermal chords and thick somatic musculature. Lateral hypodermal chords very wide; nuclei of numerous chordal cells visible. Total number of hypodermal chords not determined. In anterior end, muscular envelope having (in addition to longitudinal) diagonal and transversal muscle fibres. Somatic sensilla sparsely distributed, short, cylindrical, ca. 2.5 μm length, associated with hypodermal chords. Metanemes not found. Nerve ring situated at ca. 650 μm from head end. Caudal gland opening visible at terminal tail tip. Cephalic sensilla arranged in two circles (6 + 10). First circle represents six labial disc-shaped papilla (extremely minute) located at lip bases. Second circle consists of short cylindrical setae, four pairs of lateromedian (of them, first ca. 3 and second ca. 4–5 μm length) and two lateral setae ca. 3 μm length. Amphidial aperture small, pore-like (ca. 1–2 μm diameter), with clear prominent rim, situated at ca. 50 μm from head end. Canalis amphidialis hardly visible. Mouth opening surrounded by three lips (two subventral and one dorsal). Pharynx muscular, cylindrical. Three pharyngeal gland ducts visible in anterior pharynx, two subventral opening at terminal pharynx (ca. 5 μm from head apex) and dorsal – at ca. 10 μm posterior head apex. Cardia not seen. Intestine with visible internal lumen. Rectum hardly visible, lacking thick cuticular walls. Anus in shape of transversal slit. Ventral excretory gland opening visible on ventral side at ca. 520 μm posterior head end. Excretory gland comprises long duct and two large cellular bodies. Anterior- and posteriormost cellular bodes laying ca. 3.3 and 4.7 mm from head end. Vulva and gonads not found.

The examined juvenile definitely satisfies the morphological descriptive criteria of the family Marimermithidae. Among the distinctive features are: larval parasitic lifestyle, overall

habitus, head sensillar pattern and location, amphid structure, three mouth lips, presence of three well-developed pharyngeal glands opening very close to mouth edge[24–27]. Very short or papilloid cephalic sensilla and a two-celled excretory gland with a long duct opening anterior to nerve ring are all characteristic of the genus *Aborjinia* Özdikmen 2010 (pro *Australonema* Tchesunov et Spiridonov 1985, junior homonym of *Australonema* Tassell 1980)[25–27]. Accordingly, the examined juvenile should be attributed to the genus *Aborjinia*.

### 4.3. Specimen dentification in phanodermatid K2 isolate

Specimen K2 was a juvenile selected for sequencing from a collection containing several juvenile individuals and one mature female retrieved from the foraminifer *Reophax curtus*. The specimens had slim fusiform bodies, smooth cuticle and discernible dark oculi typical of the free-living enoplid family Phanodermatidae. Some specimens exhibited peculiar exaggerated pharyngeal glands, perhaps due to enhanced secretion during in-test association with foraminifers, and a residual gut content suggesting a non-symbiotic exploitive nature of the association. The female and juveniles could not be identified with certainty to species or genus level and are hereby designated Phanodermatidae gen. sp. (fam. Phanodermatidae Filipjev, 1927; order Enoplida Filipjev 1929).

4.3.1. Female morphology of Phanodermatidae gen. sp.

Body fusiform, with smooth cuticle. Length 3,043 μm, middle diameter 66 μm. Cephalic setae in two closely spaced circles (4 + 6), 10 and 7 μm length. Amphids small, slit-shaped, ca. 4 μm. Body diameter at amphids 15 μm. Amphideal fovea prolongation not definable. Oral cavity minute to indefinable. Three protrusions visualised in stoma. Renette small-celled, with pore opening in anterior body end, duct continuing along pharynx. Pharynx muscular with prominent transverse striation, anterior third containing nerve ring with large accompanying assemblage of neuronal bodies. Posterior pharynx contains large glandular extension with three large pharyngeal gland cell bodies, two latero-ventral and one dorsal. Body diameter at this section 73 μm. Pharyngeal glands markedly exaggerated, open anteriorly into pharynx. Gut reveals distinct cell boundaries and central lumen discernible throughout and containing nutritive content. Anus ventral posterior. Body diameter at anal orifice 56 μm. Ovaries homodromous. Vulvar opening approximately middle-body. Caudal gland cell bodies posterior, with homogeneous cytoplasm, open at tail tip.

4.3.2. Microdrawing of female Phanodermatidae gen. sp.

Left – general view, scale bar 300 µm. Right – cephalic end, scale bar 20 µm.

300µm   20µm
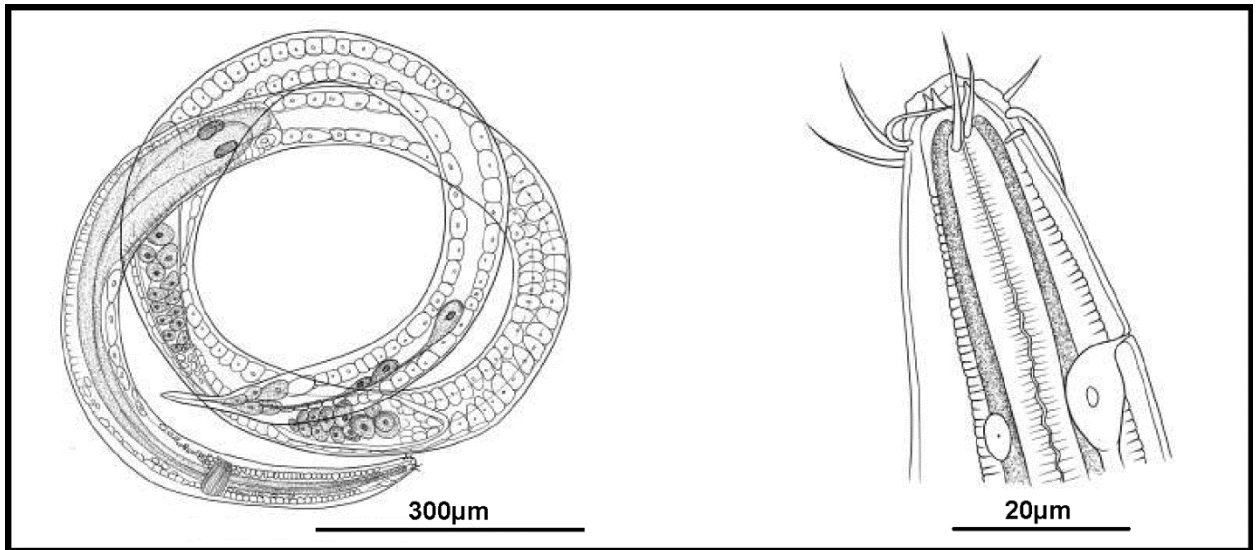
5. Supplementary references

1. Smythe, A.B., Holovachov, O., and Kocot, K.M. (2019). Improved phylogenomic sampling of free-living nematodes enhances resolution of higher-level nematode phylogeny. BMC Evol. Biol. *19*.

2. Yoder, M., Tandingan De Ley, I., King, I.W., Mundo-Ocampo, M., Mann, J., Blaxter, M., Poiras, L., and De Ley, P. (2006). DESS: A versatile solution for preserving morphology and extractable DNA of nematodes. Nematology *8*, 367–376.

3. Williams, B.D., Schrank, B., Huynh, C., Shownkeen, R., and Waterston, R.H. (1992). A genetic mapping system in *Caenorhabditis elegans* based on polymorphic sequence-tagged sites. Genetics *131*, 609–624.

4. Medlin, L., Elwood, H.J., Stickel, S., and Sogin, M.L. (1988). The characterization of enzymatically amplified eukaryotic 16S-like rRNA-coding regions. Gene *71*, 491–499.

5. van der Auwera, G., Chapelle, S., and De Wächter, R. (1994). Structure of the large ribosomal subunit RNA of *Phytophthora megasperma*, and phylogeny of the oomycetes. FEBS Lett. *338*, 133–136.

6. Bolger, A.M., Lohse, M., and Usadel, B. (2014). Trimmomatic: A flexible trimmer for Illumina sequence data. Bioinformatics *30*, 2114–2120.

7.   Martin, M. (2011). Cutadapt removes adapter sequences from high-throughput sequencing reads. EMBnet.journal *17*, 10.

8.   Bankevich, A., Nurk, S., Antipov, D., Gurevich, A.A., Dvorkin, M., Kulikov, A.S., Lesin, V.M., Nikolenko, S.I., Pham, S., Prjibelski, A.D., et al. (2012). SPAdes: A new genome assembly algorithm and its applications to single-cell sequencing. J. Comput. Biol. *19*, 455–477.

9.   Altschul, S.F., Madden, T.L., Schäffer, A.A., Zhang, J., Zhang, Z., Miller, W., and Lipman, D.J. (1997). Gapped BLAST and PSI-BLAST: A new generation of protein database search programs. Nucleic Acids Res. *25*, 3389–3402.

10.   Langmead, B., and Salzberg, S.L. (2012). Fast gapped-read alignment with Bowtie 2. Nat. Methods *9*, 357–359.

11.   Milne, I., Stephen, G., Bayer, M., Cock, P.J.A., Pritchard, L., Cardle, L., Shawand, P.D., and Marshall, D. (2013). Using tablet for visual exploration of second-generation sequencing data. Brief. Bioinform. *14*, 193–202.

12.   Katoh, K., and Standley, D.M. (2013). MAFFT multiple sequence alignment software version 7: Improvements in performance and usability. Mol. Biol. Evol. *30*, 772–780.

13.   Tabei, Y., Kiryu, H., Kin, T., and Asai, K. (2008). A fast structural multiple alignment method for long RNA sequences. BMC Bioinformatics *9*, 33.

14.   Capella-Gutiérrez, S., Silla-Martínez, J.M., and Gabaldón, T. (2009). trimAl: A tool for automated alignment trimming in large-scale phylogenetic analyses. Bioinformatics *25*, 1972–1973.

15.   Ronquist, F., Teslenko, M., van der Mark, P., Ayres, D.L., Darling, A., Höhna, S., Larget, B., Liu, L., Suchard, M.A., and Huelsenbeck, J.P. (2012). Mrbayes 3.2: Efficient bayesian phylogenetic inference and model choice across a large model space. Syst. Biol. *61*, 539–542.

16.   Gelman, A., and Rubin, D.B. (1992). Inference from iterative simulation using multiple sequences. Stat. Sci. *7*, 457–472.

17.   Nguyen, L.T., Schmidt, H.A., von Haeseler, A., and Minh, B.Q. (2015). IQ-TREE: A fast and effective stochastic algorithm for estimating maximum-likelihood phylogenies. Mol. Biol. Evol. *32*, 268–274.

18.   Kalyaanamoorthy, S., Minh, B.Q., Wong, T.K.F., von Haeseler, A., and Jermiin, L.S. (2017). ModelFinder: Fast model selection for accurate phylogenetic estimates. Nat. Methods *14*, 587–589.

19.   Tamura, K., Stecher, G., Peterson, D., Filipski, A., and Kumar, S. (2013). MEGA6: Molecular evolutionary genetics analysis version 6.0. Mol. Biol. Evol. *30*, 2725–2729.

20.   Shimodaira, H. (2002). An approximately unbiased test of phylogenetic tree selection. Syst. Biol. *51*, 492–508.

21.   Strimmer, K., and Rambaut, A. (2002). Inferring confidence sets of possibly misspecified gene trees. Proc. R. Soc. B Biol. Sci. *269*, 137–142.

22.   Kishino, H., Miyata, T., and Hasegawa, M. (1990). Maximum likelihood inference of protein phylogeny and the origin of chloroplasts. J. Mol. Evol. *31*, 151–160.

23.   Rubtzov, I.A., and Platonova, T.A. (1974). A new family of marine parasitic nematodes. Zool. Zhurnal *53*, 1445-1458. [in Russian].

24.   Tchesunov, A. V. (1997). On the histological anatomy of *Marimermis maritima* Rubzov & Platonova, 1974 (Nematoda: Enoplia: Marimermithida), parasite of a sea urchin. Fundam. Appl. Nematol. *20*, 349–356.

25.   Tchesunov, A. V., and Spiridonov, S.E. (1985). *Australonema eulagiscae* gen. et sp. n. (Nematoda, Marimermithida), a parasite of a polychete from Antarctics. Vestn. Zool. *2*, 16-21. [in Russian].

26.   Miljutin, D.M. (2003). Histological studies on the anatomy of the parasitic stages of *Australonema* sp. (Nematoda: Marimermithida). Nematology *5*, 275–291.

27.   Miljutin, D.M. (2014). Order Marimermithida Rubtzov 1980, emend. Tchesunov 1995. In Handbook of Zoology. Gastrotricha, Cycloneuralia and Gnathifera. Volume 2: Nematoda, A. Schmidt-Rhaesa, ed. (De Gruyter), pp. 345–350.